

Generation of a sub-Poissonian state with quantum high- and low-pass filters

Hai-bo Wang,* Yongmin Li,† Satoru Odate, and Takayoshi Kobayashi

Core Research for Evolutional Science and Technology (CREST), Japan Science and Technology Corporation (JST),
Department of Physics, Graduate School of Science, University of Tokyo, 7-3-1 Hongo, Bunkyo, Tokyo 113-0033, Japan

(Received 8 March 2005; published 27 July 2005)

We introduce a quantum component, the *quantum high- and low-pass filter*, and analyze its output characteristic. It is shown that a quantum bandpass filter can be achieved by using passive linear optics and projection measurements. Furthermore, we show that the sub-Poissonian state can be generated by using a cascaded quantum low-pass filter and high-pass filter.

DOI: [10.1103/PhysRevA.72.013822](https://doi.org/10.1103/PhysRevA.72.013822)

PACS number(s): 42.50.Ar, 42.50.Dv

Since Hollenhorst and Caves [1] introduced the concept of a squeezed state, it has been widely used in quantum optics and in many other branches of quantum physics, from solid-state physics to cosmology [2]. Recently, quantum entanglement, which can be generated from squeezed states [3], has played an essential role in quantum information and communication. Many different schemes of generating squeezed states were proposed and experimentally realized, such as optical parametric amplification [4], resonance fluorescence [5], harmonic generation [6], etc. The squeezed state had also been applied to experimental demonstration of high-sensitivity measurements [7], quantum nondemolition (QND) measurements [8], construction of quantum networks [9], etc. until now, all of the proposed or realized squeezed states were built on nonlinear physics processes [10].

Recently, significant progress has been achieved by proposals for quantum gates using only passive linear optics and projection measurements [11–13]. These proposals show that strong nonlinear effects can be implemented by exploiting post-selection strategies based on single-photon technologies [14]. For example, the nonlinear π -phase shift and controlled-NOT quantum gate have been experimentally demonstrated by using linear optics components [15,16]. In a similar way, entanglement concentration and entanglement purification can be achieved by using conditional measurements [17].

To date, the nonlinear effect caused by linear optics and projection measurement has been limited in the discrete variable of quantum optics and quantum information, so that it may be interesting to extend this technique to the continuous-variable regime. In this paper, we introduce a quantum component, the *quantum high- and low-pass filter* (*quantum HPF and LPF*), which consists of linear optics components. We analyze the output characteristic of the quantum filter and show that it is possible to generate a squeezed state by assembling linear optics components.

Figure 1 shows the optical circuit of a quantum filter. A similar setup has been used to demonstrate the QND measurement of the Fock states [18,19]. We analyze the circuit

for an arbitrary input state and show how it can work as a quantum filter. Beam splitters *A*, *B*, and *C* shown in Fig. 1 are assumed to be asymmetric in phase. The reflection off the “dashed” surface of each beam splitter produces a sign change. The operator input-output relations between the two input modes (a_{in}, b_{in}) and the corresponding output modes (a_{out}, b_{out}) have the general form $a_{out} = \sqrt{\eta_i} a_{in} + \sqrt{1 - \eta_i} b_{in}$ and $b_{out} = \sqrt{1 - \eta_i} a_{in} - \sqrt{\eta_i} b_{in}$, where η_i and $1 - \eta_i$ are the intensity reflectivity and transmittivity. $i = a, b$, and c correspond to beam splitters *A*, *B*, and *C*, respectively. The crucial component in this interferometer is beam splitter *C*, which is used to achieve the nonlinear π -phase-shift operation [15,20]. In this paper, we consider only cases where one of the detectors D_{b2} and D_{c2} counts one photon and only one photon (OPOOP) and another detector counts no photons. Provided the photons are indistinguishable, the occurrence of conditional interference depends on the input photon number. The phase of photon state in beam *t* depends on the incident photon number n and the reflectivity η_c [15]. For $n < \eta_c / (1 - \eta_c)$, no phase shift occurs, and for $n > \eta_c / (1 - \eta_c)$, it picks up a π -phase shift.

The application of the filter to a Fock state provides a definite output. Let the Fock state $|n_w\rangle$ impinge on the input ports a_1 . A single-photon state $|1\rangle$ is injected into the ancilla mode b_1 and the other ancilla mode c_1 is unoccupied. The reflectivities of each beam splitters are set by

$$\eta_a = 1/(n_w + 1)(1 - \eta_c), \quad \eta_b = \eta_c/n_w(1 - \eta_c),$$

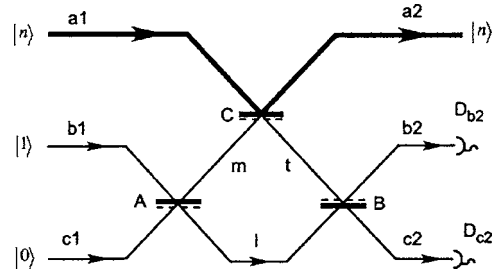


FIG. 1. Optical circuit of a quantum filter. Beam splitters *A*, *B*, and *C* are assumed to be asymmetric in phase. Reflection off the “dashed” surface of each beam splitter produces a sign change. D_{b2} and D_{c2} are single-photon detectors. The quantum filter is realized when the detectors D_{b2} and D_{c2} count one photon and only one photon and another detector counts no photon. b_1 and c_1 are ancilla modes.

*Electronic address: wang@femto.phys.s.u-tokyo.ac.jp

†Current address: Institute of Opto-Electronics, Shanxi University, China.

$$0 < \eta_c < n_w/(n_w + 1). \quad (1)$$

The conditional interference of the filter can be maximized by setting η_a and η_b to satisfy Eq. (1). So that, if n_w photons exist in path a_1 , a π -phase shift occurs for state in path t and one photon will appear at port c_2 . On the contrary, if no photons are in path a_1 , no phase shift occurs in path t and the single photon appears at output port of b_2 . These operations succeed with 100% probability. For convenience, the point n_w is called the *working point*. Therefore, the QND of the n_w state will be achieved when one photon appears at output port c_2 [18].

When photons with a different number from n_w are injected into this scheme, the output is not so clear and QND cannot be achieved. Next, we consider the output characteristic of this scheme for a generalized input state and show that this scheme may be treated as a quantum HPF or LPF. The input state at the port a_1 may be expanded in terms of the number states as $|\Psi\rangle_{a_1} = \sum C_n |n\rangle_{a_1}$. The input state for the quantum filter is given by $|\psi_{in}\rangle = \sum_{n=0}^{\infty} C_n |n\rangle_{a_1} |1\rangle_{b_1} |0\rangle_{c_1}$. The reflectivities of each beam splitter are set as Eq. (1). After passing through the setup, the output state becomes

$$\begin{aligned} & \sum_{n=0}^{\infty} \sqrt{\eta_c}^{n-1} C_n \{ [\sqrt{\eta_c(1-\eta_a)(1-\eta_b)} - (n-n\eta_c-\eta_c) \sqrt{\eta_a\eta_b}] \\ & \times |n\rangle_{a_2} |1\rangle_{b_2} |0\rangle_{c_2} + [\sqrt{\eta_c(1-\eta_a)\eta_b} + (n-n\eta_c-\eta_c) \\ & \times \sqrt{\eta_a(1-\eta_b)}] |n\rangle_{a_2} |0\rangle_{b_2} |1\rangle_{c_2} \}. \end{aligned} \quad (2)$$

One may use the technique of conditional-state preparation [21], in which the state is extracted by a triggering signal. In our case, the triggering signal is one of the detectors D_{b_2} and D_{c_2} counts OPOOP while another detector counts no photons. Depending on the triggering signal, the filter will work as a quantum HPF or LPF. For example, when the detector D_{c_2} counts OPOOP and the detector D_{b_2} counts no photons, the output state is reduced to the second part of Eq. (2),

$$\begin{aligned} |\psi_{out}\rangle_{HPF} = & \sum_{n=0}^{\infty} \sqrt{\eta_c}^{n-1} C_n \{ [\sqrt{\eta_c(1-\eta_a)\eta_b} + (n-n\eta_c-\eta_c) \\ & \times \sqrt{\eta_a(1-\eta_b)}] |n\rangle_{a_2} |0\rangle_{b_2} |1\rangle_{c_2} \}, \end{aligned} \quad (3)$$

and the first part of Eq. (2) is discarded by post-selection. Line 1 in Fig. 2(a) shows how the normalized output probability of the filter varies with photon number. The parameters are set to $n_w=30$ and $\eta_c=n_w/(n_w+1)-0.3$. It can be seen that curve 1 in Fig. 2(a) shows a typical response like a classical HPF. In this way, a quantum HPF is realized in a quantum domain. The output characteristic of the quantum filter can be improved by using second- or higher-order quantum HPF. The simplest way to make a second-order filter is just to cascade two quantum filters—that is, to connect one after the other, so the input state must go through the first one and then the second. Line 3 in Fig. 2(a) shows the response for third-order quantum HPF. It can be seen that the slope of line 3 are steeper than the first-order one. Therefore, a quantum HPF can be achieved by only linear optics and conditional-state preparation. When the detector D_{b_2} counts OPOOP and the detector D_{c_2} counts no photons, the filter is

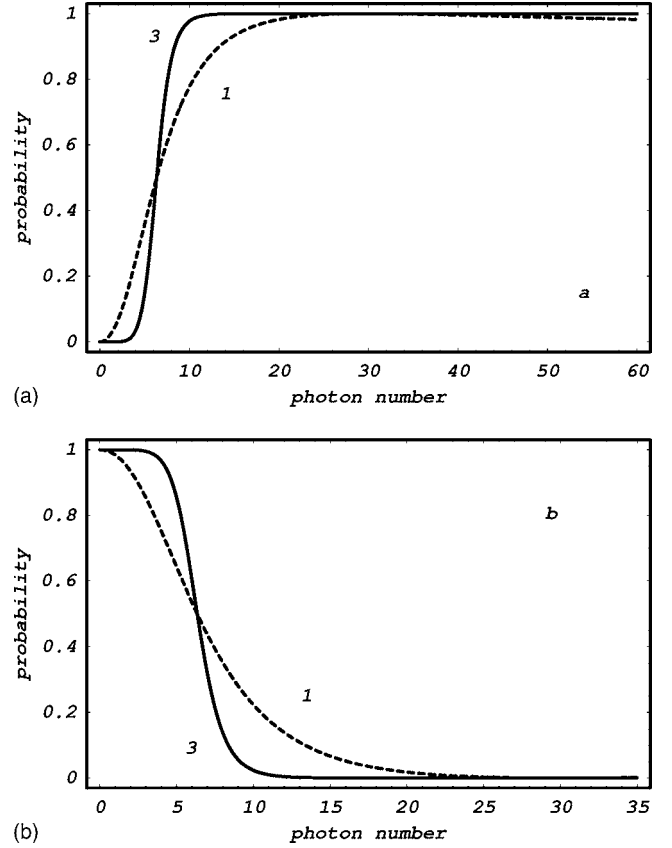


FIG. 2. The response of quantum HPF and LPF. (a) The typical response of a quantum HPF when the detector D_{c_2} counts OPOOP and detector D_{b_2} counts no photons. Lines 1 and 3 correspond to first- and third-order HPF. (b) The response of a quantum LPF when the detector D_{b_2} counts OPOOP and detector D_{c_2} counts no photons. Lines 1 and 3 correspond to first- and third-order LPF. The parameters are set to be $n_w=30$, $\eta_c=n_w/(n_w+1)-0.3$.

worked as a quantum LPF and the response graphs are shown in Fig. 2(b). The third-order quantum LPF is also shown in Fig. 2(b).

The clearest physical description of the quantum filter properties is that of a QND measurement for the n -photon state. At the working point of $n=n_w$, the quantum filter can be perfectly demonstrated. The imperfect QND measurement provides the response function of a quantum HPF or LPF. It should be pointed out that the quantum filter, shown in our paper, is different from a classical filter. The response of the classical filter has a definite value for each input physical quantity. However, the curves shown in Fig. 2 compose a probability distribution function for each input photon number, which gives the conditional probability that the photons appear at the output port a_2 of the filter while the triggering signal happens. This filter can thus be used to generate a sub-Poissonian state which is generally generated from non-linear process before.

Consider the schematic setup for generation of the sub-Poissonian state illustrated in Fig. 3. The input state $|\psi_{in}\rangle = |\alpha\rangle$ for the setup is a coherent state, which can be written as a superposition of Fock states in the form

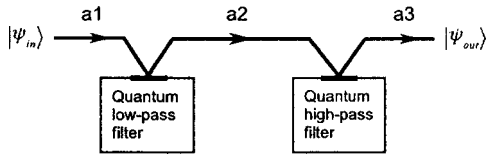


FIG. 3. Schematic for the generation of sub-Poissonian state. The coherent state passes through a quantum LPF firstly and then a quantum HPF. The quantum LPF and HPF may have different working points n_1 and n_2 .

$$|\alpha\rangle = e^{-|\alpha|^2/2} \sum_{m=0}^{\infty} \frac{\alpha^m}{\sqrt{m!}} |m\rangle. \quad (4)$$

The coherent state passes through a quantum LPF first and then a quantum HPF. The quantum LPF and HPF may have different working points n_1 and n_2 . The sub-Poissonian-state preparation is successful when the operations of both quantum filters work properly. The output state can then be derived as

$$\begin{aligned} |\psi_{out}\rangle = & e^{-|\alpha|^2/2} \sum_{m=0}^{\infty} \frac{\alpha^m}{\sqrt{m!}} \sqrt{\eta_{c1}}^{m-1} \sqrt{\eta_{c2}}^{m-1} \\ & \times [\sqrt{\eta_{c1}(1-\eta_{a1})(1-\eta_{b1})} \\ & - (m-m\eta_{c1}-\eta_{c1})\sqrt{\eta_{a1}\eta_{b1}}] \\ & \times [\sqrt{\eta_{c2}(1-\eta_{a2})\eta_{b2}} \\ & + (m-m\eta_{c2}-\eta_{c2})\sqrt{\eta_{a2}(1-\eta_{b2})}] |m\rangle. \quad (5) \end{aligned}$$

Figure 4 shows an example that generates a sub-Poissonian state for a specific case of this scheme. The input light is a coherent state with $|\alpha| = \sqrt{2}$. The solid line in Fig. 4 gives the probability distribution of the state $|\psi_{out}\rangle$ after the filter pair. The Poissonian distribution $P(m)$ of a coherent state is also shown in Fig. 4 (dashed line). For convenience, the probability distribution of the sub-Poissonian state has been magnified to the same level as the coherent state. It can be seen that the width of photon-number distribution of $|\psi_{out}\rangle$ is much

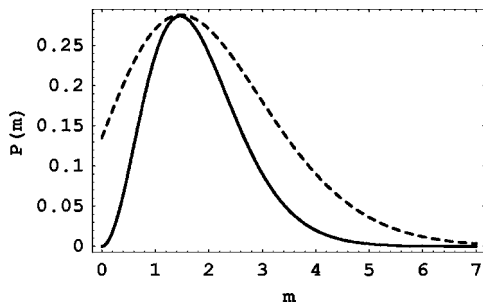


FIG. 4. The distribution function $P(m)$ of the generated sub-Poissonian state for a specific case of this scheme. The solid line gives the probability distribution of the state $|\psi_{out}\rangle$ after the filter pair. The dashed line shows the Poissonian distribution of a coherent state with $|\alpha| = \sqrt{2}$. The parameters are set to be $n_1=20$, $n_2=10$, $\eta_{c1}=n_1/(n_1+1)-0.4$, and $\eta_{c2}=n_2/(n_2+1)-0.4$.

narrower than that of the coherent state. The parameters are set to be $n_1=20$, $n_2=10$, $\eta_{c1}=n_1/(n_1+1)-0.4$, and $\eta_{c2}=n_2/(n_2+1)-0.4$. The efficiency of successful sub-Poissonian-state preparation in our scheme can be defined as the ratio between the post-selected photons and the injected coherent photons. The probability of the sub-Poissonian state shown in Fig. 4 can be calculated to be 1.3%, which is a receivable level. More squeezing of the photon-number distribution with reduced successful probability can be realized by using higher-order LPF and HPF.

It should be noted that the quantum filter, as depicted in our paper, is a nondeterministic quantum element, the operation of which is conditioned on the detection of an auxiliary photon. The generation of the sub-Poissonian state can be seen as a collapse of the entanglement among photons at the output ports of a_2 , b_2 , and c_2 . However, the state preparation is made by post-selection of the relevant events in the record of the measurements on the two detectors, which can be made after the end of the physical measurement. In fact, due to the fact that only one photon exists at the output ports of b_2 or c_2 , all n -photon components which happen to appear at the output port a_2 will contribute to the non-post-selected output state, so that no wave-function collapse actually occurs from the non-post-selected output state to the sub-Poissonian state.

In our proposal, the single-photon detector is idealized which can distinguish one photon from a vacuum and multiphotons. Further developments are expected for detectors with such a capability. Takeuchi *et al.* [14] described a single-photon resolution detector that can distinguish between one and two photons very well, but the quantum efficiency of this detector is presently limited to 88%. This means that there is a chance of mistakenly identifying a two-photon state as a single-photon state. Also, the dark count rate of photodetectors will strongly affect the quality of the sub-Poissonian state. At present, the major technological challenge is to improve the quantum efficiency of detectors to distinguish single-photon events from two-photon and zero-photon events.

In conclusion, we first introduced and analyzed the output characteristic of quantum high- and low-pass filters which consist of only passive linear optics. It was shown that a sub-Poissonian state can be generated from a coherent state by using a bandpass filter which consists of quantum LPF and HPF. The generated sub-Poissonian state in a free-propagating optical mode can then be used for other purposes. The difference between our scheme and those proposed before was that the measurement-caused nonlinear effect, instead of the traditional nonlinear process, is used to alter the photon distribution of a coherent light. Closer to our proposal, Sanaka [18] suggested a scheme to generate photon-number Fock states by a chain of beam splitters and quantum nondemolition measurements. However, the proposed scheme is relative inefficient due to many beam splitters and post-selection by many single-photon detectors. In our scheme, it is enough to generate a sub-Poissonian state by just two quantum filters. The complicated multiphoton interference has been removed so that the efficiency of state preparation has been much improved.

- [1] J. N. Hollenhorst, *Phys. Rev. D* **19**, 1669 (1979); C. M. Caves, *ibid.* **23**, 1693 (1981).
- [2] W. M. Zhang, D. H. Feng, and R. Gilmore, *Rev. Mod. Phys.* **62**, 867 (1990); V. V. Dodonov, *J. Opt. B: Quantum Semiclassical Opt.* **4**, R1 (2002); R. Loudon and P. L. Knight, *J. Mod. Opt.* **34**, 709 (1987).
- [3] M. D. Reid and P. D. Drummond, *Phys. Rev. Lett.* **60**, 2731 (1988); P. van Loock and A. Furusawa, *Phys. Rev. A* **67**, 052315 (2003); T. Aoki, N. Takei, H. Yonezawa, K. Wakui, T. Hiraoka, A. Furusawa, and P. van Loock, *Phys. Rev. Lett.* **91**, 080404 (2003); J. Jing *et al.*, *ibid.* **90**, 167903 (2003).
- [4] L. A. Wu, H. J. Kimble, J. L. Hall, and H. Wu, *Phys. Rev. Lett.* **57**, 2520 (1986); X. J. Jia, X. L. Su, Q. Pan, J. R. Gao, C. D. Xie, and K. C. Peng, *ibid.* **93**, 250503 (2004); W. P. Bowen, N. Treps, B. C. Buchler, R. Schnabel, T. C. Ralph, Hans-A. Bachor, T. Symul, and P. K. Lam, *Phys. Rev. A* **67**, 032302 (2003).
- [5] D. F. Walls and P. Zoller, *Phys. Rev. Lett.* **47**, 709 (1981).
- [6] L. Mandel, *Opt. Commun.* **42**, 437 (1982); Z. H. Zhai, Y. M. Li, and J. R. Gao, *Phys. Rev. A* **69**, 044301 (2004); Ulrik L. Andersen and Preben Buchhave, *J. Opt. Soc. Am. B* **20**, 1947 (2003); P. Lodahl, *Phys. Rev. A* **68**, 023806 (2003).
- [7] E. S. Polzik, J. Carri, and H. J. Kimble, *Phys. Rev. Lett.* **68**, 3020 (1992); K. McKenzie, D. A. Shallock, D. E. McClelland, B. C. Buchler, and P. K. Lam, *Phys. Rev. Lett.* **88**, 231102 (2002).
- [8] P. Grangier, J. A. Levenson, and J.-P. Poizat, *Nature (London)* **396**, 537 (1998); H. Wang, Y. Zhang, Q. Pan, H. Su, A. Porzio, C. Xie, and K. Peng, *Phys. Rev. Lett.* **82**, 1414 (1999).
- [9] H. Yonezawa, T. Aoki, and A. Furusawa, *Nature (London)* **431**, 430 (2004).
- [10] The Schrödinger cat state without a squeezed state, which is a quantum superposition of macroscopic system, was proposed to generate from only linear optics and projection measurements. See A. P. Lund, H. Jeong, T. C. Ralph, and M. S. Kim, *Phys. Rev. A* **70**, 020101(R) (2004). However, no one showed that a squeezed state can be generated from linear optics systems and projection measurements.
- [11] E. Knill, R. Laflamme, and G. Milburn, *Nature (London)* **409**, 46 (2001).
- [12] T. C. Ralph, A. G. White, W. J. Munro, and G. J. Milburn, *Phys. Rev. A* **65**, 012314 (2001); T. C. Ralph, N. K. Langford, T. B. Bell, and A. G. White, *ibid.* **65**, 062324 (2002).
- [13] H. F. Hofmann and S. Takeuchi, *Phys. Rev. Lett.* **88**, 147901 (2002); X. B. Zou, K. Pahlke, and W. Mathis, *Phys. Rev. A* **66**, 064302 (2002); A. Grudka and A. Wojcik, *ibid.* **66**, 064303 (2002).
- [14] S. Takeuchi *et al.*, *Appl. Phys. Lett.* **74**, 1063 (1999); B. Lounis and W. E. Moerner, *Nature (London)* **407**, 491 (2000); J. Kim, S. Takeuchi, Y. Yamamoto, and H. H. Hogue, *Appl. Phys. Lett.* **74**, 902 (1999).
- [15] Kaoru Sanaka, Thomas Jennewein, Jian-Wei Pan, Kevin Resch, and Anton Zeilinger, *Phys. Rev. Lett.* **92**, 017902 (2004).
- [16] T. B. Pittman, M. J. Fitch, B. C. Jacobs, and J. D. Franson, *Phys. Rev. A* **68**, 032316 (2003); Zhi Zhao, An-Ning Zhang, Yu-Ao Chen, Han Zhang, Jiang-Feng Du, Tao Yang, and Jian-Wei Pan, *Phys. Rev. Lett.* **94**, 030501 (2005).
- [17] Z. Zhao, T. Yang, Y. A. Chen, A. N. Zhang, and J. W. Pan, *Phys. Rev. Lett.* **90**, 207901 (2003); J. W. Pan *et al.*, *Nature (London)* **423**, 417 (2003); T. Yamamoto, M. Koashi, and N. Imoto, *Phys. Rev. A* **64**, 012304 (2001); T. Yamamoto *et al.*, *Nature (London)* **42**, 343 (2003).
- [18] K. Sanaka, *Phys. Rev. A* **71**, 021801(R) (2005).
- [19] G. J. Pryde, J. L. O'Brien, A. G. White, S. D. Bartlett, and T. C. Ralph, *Phys. Rev. Lett.* **92**, 190402 (2004).
- [20] H. B. Wang and T. Kobayashi, *Phys. Rev. A* **71**, 021802(R) (2005).
- [21] J. Laurat, T. Coudreau, N. Treps, A. Maitre, and C. Fabre, *Phys. Rev. Lett.* **91**, 213601 (2003); J. Laurat, T. Coudreau, N. Treps, A. Maitre, and C. Fabre, *Phys. Rev. A* **69**, 033808 (2004); Y. Zhang, K. Kasai, and M. Watanabe, *Opt. Lett.* **27**, 1244 (2002).